Optics Communications 309 (2013) 121–126

Contents lists available at ScienceDirect

Optics Communications

journal homepage: www.elsevier.com/locate/optcom

Design of an off-axis helmet-mounted display with freeform surface described by radial basis functions

Hua Li [a,b,*], Xin Zhang [a], Chao Wang [a,b], Jianping Zhang [a], Lingjie Wang [a], Hemeng Qu [a]

[a] Key Laboratory of Optical System Advanced Manufacturing Technology, Changchun Institute of Optics, Fine Mechanics and Physics, Chinese Academy of Sciences, Changchun 130033, China

[b] University of Chinese Academy of Sciences, Beijing 100039, China

ARTICLE INFO

Article history:
Received 21 March 2013
Received in revised form
25 June 2013
Accepted 26 June 2013
Available online 18 July 2013

Keywords:
Optical design
Displays
Freeform surface
Radial basis functions
Binary optics

ABSTRACT

An off-axis optical system with a freeform surface described by Gaussian radial basis functions for a see-through wide field of view helmet-mounted display (HMD) is presented. By using a freeform surface, an off-axis see-through HMD system with one tilted freeform combiner and four relay optical lenses is designed. An off-axis see-through wide field of view HMD system with a 100 mm eye relief, 15 mm pupil, $45^\circ \times 32^\circ$ FOV, and 60° combiner tilt angle is achieved. For the purpose of comparison, two other off-axis see-through HMDs which have the same specifications, but different surface type of combiner and different use count of relay lenses are designed too. One of the two contributions in this paper is the application of radial basis functions to describe optical freeform surface in a wide field of view off-axis helmet-mounted displays, and the other is a way used to determine a starting point of optimization quickly while designing.

1. Introduction

The official history of helmet-mounted display (HMD) starts almost a century ago, with Albert Bacon Pratt, of Lyndon, Vermont [1], and the development of HMD opens with this pioneering exploration and experiment. Design of a HMD involves many principles such as optical engineering, optical material, optical coating, electronics, manufacturing technology, ergonomics, etc. HMD has come a long way from its origin, but more compact structure and lighter weight are still the goal of designers. To achieve the above mentioned deign target, researchers have made unremitting efforts. Besides, there have been many advances in some ways—light source, optical design and manufacturing, and so on. With incessant requirements for high performance, more and more new techniques and new components have been applied to the design of HMD. Many optical systems for see-through HMD have been reported in the past few years.

Rolland designed a 60° field of view optical see-through head-mounted display using off-axis configuration [2]. A breakthrough in the weight reduction challenge was the work of Chen who developed a helmet visor display using diffractive optical elements (DOE) [3]. BAE Systems has exploited Holographic Optical Waveguide technology in Q-Sight^{TM} family of scalable Helmet-Mounted Displays [4]. With the advent of diamond turning technology which can manufacture polygon and optical freeform surface, people begin to research new mathematical descriptions of freeform surface. Examples of freeform surface descriptions include x–y polynomials [5], Zernike polynomials [6], and φ-polynomials [7]. There is a new way to describe freeform surfaces with radial basis functions (RBF), a meshless surface description first applied to optical system design by Cakmakci et al.

Cakmakci et al. in 2008, proposed and implemented a local optical surface representation as a sum of a linear combination of basic functions. As a design example, a single surface off-axis magnifier with a >15 mm eye relief, 3 mm pupil, and 24° diagonal full field of view was designed [8]. Furthermore, they gave another report that the radial basis function was used to describe a freeform mirror in a dual-element off-axis magnifier with a12 mm exit pupil, 15.5 mm eye clearance, and 20° diagonal full field of view in the same year [9]. Improvement of theory and promotion of application in this field will benefit a lot for optical engineering. So, we design a HMD with large field of view, large pupil size, and long exit pupil relief through the use of freeform surface described by Gaussian radial basis functions.

In this paper, an off-axis see-through helmet-mounted displays that is made up of tilted combiner with a radial basis functions surface representation is achieved. Two other combiners that are described with a 10th order asphere and a 25th order Zernike

* Corresponding author at: Key Laboratory of Optical System Advanced Manufacturing Technology, Changchun Institute of Optics, Fine Mechanics and Physics, Chinese Academy of Sciences, Changchun 130033, China. Tel.: +86 13756168912; fax: +86 043186708669.
E-mail address: gdgxlh@163.com (H. Li).

0030-4018/$ - see front matter © 2013 Elsevier B.V. All rights reserved.
http://dx.doi.org/10.1016/j.optcom.2013.06.054

polynomial are used for comparison. Each system under comparison has a 100 mm eye relief, 15 mm pupil, a $45^\circ \times 32^\circ$ FOV, and a 60° combiner tilt angle.

2. Optical freeform surface representation with radial basis functions

A radial basis function [10] is any function that has a radial symmetry and typically takes the form:

$$z(\mathbf{x}) = \sum_{i=1}^{N} w_i \phi \|(\mathbf{x}-\mathbf{C}_i)\|, \tag{1}$$

Where w_i represents a coefficient in R to be determined, ϕ is a radial basis function whose form is to be selected, the distance matrix $\|\mathbf{x}-\mathbf{C_i}\|$ presents a choice on the locations and the spatial distributions of both the datasites and the basis centers; $\mathbf{C_i}$ represents a point, or a "center" in R^T whose position is to be determined, and $\|.\|$ represents the traditional Euclidean norm; there are N "centers" (N must also be determined). In some cases this form is augmented by adding a sum of polynomial terms. We approximate an optical surface Z by taking a linear combination of basis functions added to a base conic as

$$Z = \frac{cr^2}{1+\sqrt{1-(1+k)c^2r^2}} + \sum_{i=1}^{N} w_i \phi(\|\mathbf{x}-\mathbf{C_i}\|). \tag{2}$$

Radial basis functions have typically taken one of the following forms: linear, cubic, the thin-plate spline, Gaussian, multiquadric and inverse multiquadric. The Gaussian function has the following advantages that are: simple mathematical form, radial symmetry, smoothness and good analyticity of solution. In this paper, we designed the helmet-mounted display with Gaussian. Let's suppose that the number of input samples which are represented by $\mathbf{C_i}$ is N and the corresponding targets in output space is $\mathbf{d}_N$

$$\begin{aligned}
&\sum_{i=1}^{N} w_1 \phi \|(x_1-\mathbf{C}_i)\| = d_1 \\
&\sum_{i=2}^{N} w_2 \phi \|(x_2-\mathbf{C}_i)\| = d_2 \\
&\vdots \\
&\sum_{i=1}^{N} w_N \phi \|(x_N-\mathbf{C}_i)\| = d_N,
\end{aligned} \tag{3}$$

then, the above equations can be rewritten as follows:

$$\begin{bmatrix} \phi_{11} & \phi_{12} & \cdots & \phi_{1N} \\ \phi_{21} & \phi_{22} & \cdots & \phi_{2N} \\ \vdots & \vdots & & \vdots \\ \phi_{N1} & \phi_{N2} & \cdots & \phi_{NN} \end{bmatrix} \begin{bmatrix} w_1 \\ w_2 \\ \vdots \\ w_N \end{bmatrix} = \begin{bmatrix} d_1 \\ d_2 \\ \vdots \\ d_N \end{bmatrix}, \tag{4}$$

where

$$\phi_{ji} = \phi(||\mathbf{x}_j-\mathbf{C}_i||), (j,i) = 1,2\ldots N, \tag{5}$$

let

$$\begin{aligned}
&\boldsymbol{d} = [d_1, d_2 \ldots d_N]^T, \\
&\boldsymbol{W} = [w_1, w_2 \ldots w_N]^T,
\end{aligned} \tag{6}$$

and

$$\boldsymbol{\Phi} = \{\phi_{ji} | (j,i) = 1,2\ldots N\}. \tag{7}$$

Rewrite Eq. (4) as:

$$\boldsymbol{\Phi}\mathbf{W} = \mathbf{d}. \tag{8}$$

A Radial Basis Function Network (RBFN) that is used to represent a freeform optical combiner in this paper consists of three layers, as shown in Fig. 1. The connection weight vectors of the input and output layers are denoted as $\boldsymbol{\mu}$ and $\mathbf{W}$, respectively.

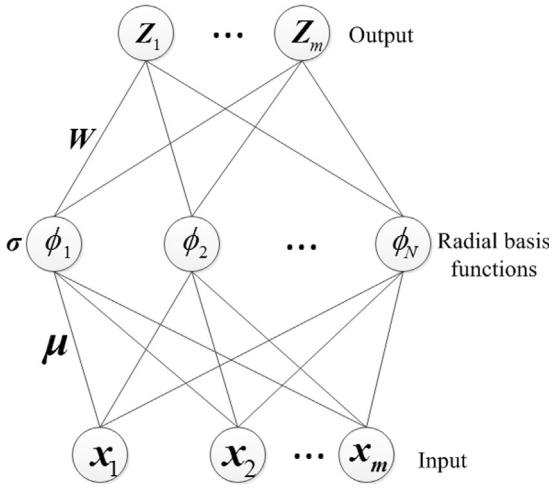

Fig. 1. A Radial Basis Function Network consisting of input nodes, hidden nodes, and output nodes. $\boldsymbol{\mu}$ is stored in the links from the input to hidden layer. σ is the normalization parameter vector of the hidden node activation functions. $\mathbf{W}$ represents the weights of links from the hidden to output layer.

The first layer consists of the input nodes, which are the x and y locations along the aperture. The basis functions in the hidden layer produce a localized response to the input stimulus. The output nodes form a weighted linear combination of the basis functions computed by the hidden nodes. The output ϕ_i of the ith hidden node, using the Gaussian kernel function as a basis, is given by

$$\phi_i = \exp\left[-\frac{(\mathbf{x}-\boldsymbol{\mu}_i)^T(\mathbf{x}-\boldsymbol{\mu}_i)}{2\sigma_i^2}\right], \; i = 1,2\ldots N, \tag{9}$$

Where $\mathbf{x}$ is the input pattern, $\boldsymbol{\mu}_i$ is its input weight vector (i.e. the center of the Gaussian for node i) and σ_i^2 is the normalization parameter, such that $0 \le \phi_i \le 1$ (the closer the input is to the center of the Gaussian, the larger the response of the node).

According to Fig. 1, the output $\mathbf{Z}$ is the resulting surface which can be represented in matrix form as Eq. (8):

$$\boldsymbol{\Phi}\mathbf{W} = \mathbf{Z}. \tag{10}$$

3. Design of an off-axis see-through wide field of view HMD optical system

3.1. Display system specifictions

We designed an off-axis see-through wide field of view HMD which comprises an image source, a relay group made of optical elements transparent to the display wavelength, and a catadioptric combiner that was described with the Gaussian radial basis functions. A diagonal 0.6″ (1.55 cm) Emagin Organic Light Emitting Diode (OLED) was selected as the image source, with a resolution of 800×600 pixels and a 15 μm pixel size. It yields a Nyquist frequency of 33 cycles/mm. A large exit pupil is important for a flight HMD, so the user will not lose the image if the HMD shifts on his head. A value of 15 mm has been deemed to be an acceptable value for these applications. The eye relief is an obvious characteristic of our design, using a value of 100 mm. This distance is sufficient to allow use of corrective spectacles, nuclear, biological and chemical (NBC) protective masks, and oxygen mask, as well as, to accommodate the wide variations in head and facial anthropometry. Furthermore, the HMD was optimized for a rectangular FOV of $45^\circ \times 32^\circ$ and the bend angle used to fold the light path back to the relay lens and the image source was chosen to be 60°. Specifications of the optical system are listed in Table 1.

3.2. Design and optimization

For the purpose of comparison, two other off-axis see-through WFOV HMD optical systems which had the same specifications as Table 1 were designed at first.

Table 1
Design specification of the off-axis see-through HMDs.

Parameter	Specification
Image source	
Microdisplay	OLED
Size	0.61″ (1.55 cm) diagonal
Active area	12.7 mm × 9.0 mm
Resolution	800 × 600 pixels
Relay lens	
Configuration	Off-axis configuration
Exit pupil diameter	15 mm
Effective focus length	21.31 mm
F-number	1.42
Eye relief	100 mm
Other system parameters	
Field of view	45° × 32°
Wavelength range	656–486 nm
Vignetting	< 10% over entire FOV

Layout of the first one is shown Fig. 2(a). The HMDs includes a combiner that is a 10th order aspherical surface and five relay lenses consisting of a doublet lens, a positive meniscus lens, a biconvex lens, and an optical wedge, arranged sequentially from the combiner to the image source.

The design strategies [11] to correct aberrations of the above HMDs optical system are as follows: (a) use an aspherical combiner surface shape to reduce bias aberration such as axial coma and binodal astigmatism; (b) tilt and decenter relay lens group to reduce perspective distortion, linear and binodal astigmatism; (c) use a wedge to reduce axial coma introduced by the tilted combiner; and (d) use a diffractive optical element to achieve the correction of primary and secondary chromatic aberration, spherochromatism and higher order aberration in highly efficient manner that allows weight reduction and also improves the color bandwidth of the HMDs. In this optical system, the second surface of the biconvex lens is a diffractive surface described as

$$\varphi(x,y) = k\frac{2\pi}{\lambda}\sum_{i=1}^{m} A_i x^j y^n,$$

$$i = \frac{1}{2}\left[(j+n)^2 + j + 3n\right], \tag{11}$$

Where k is the diffracted order, m is the number of polynomial coefficients in the series and A_i is the coefficient on the ith polynomial term. According to the given value of i, we can get

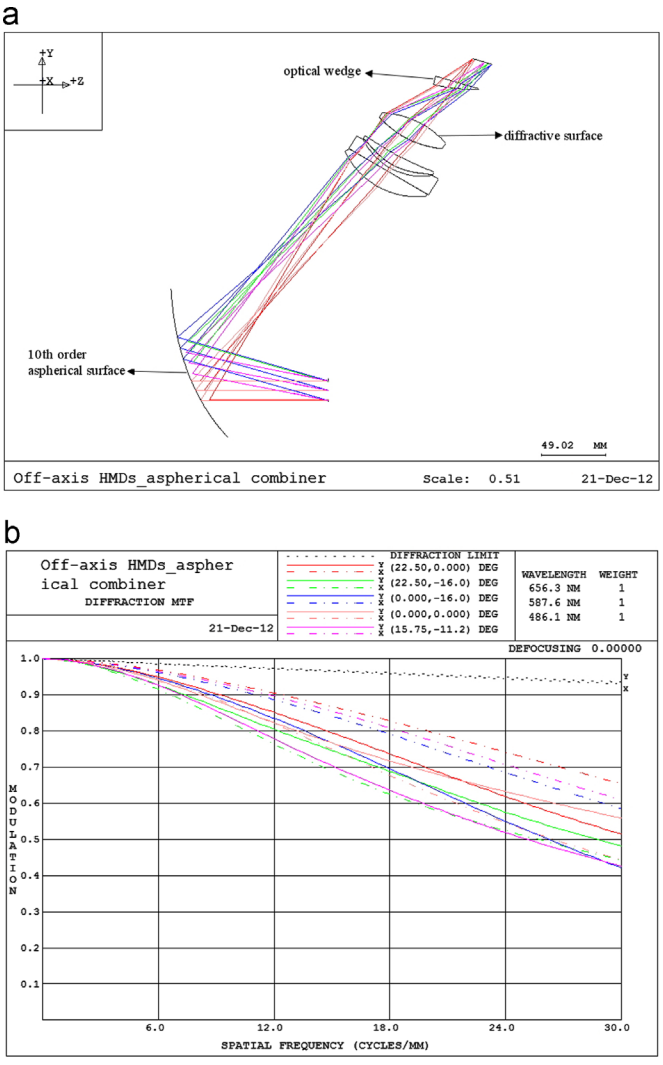

Fig. 2. (a) Optical layout of the off-axis HMDs with an aspherical combiner. (b) Polychromatic MTF plot of the off-axis HMDs.

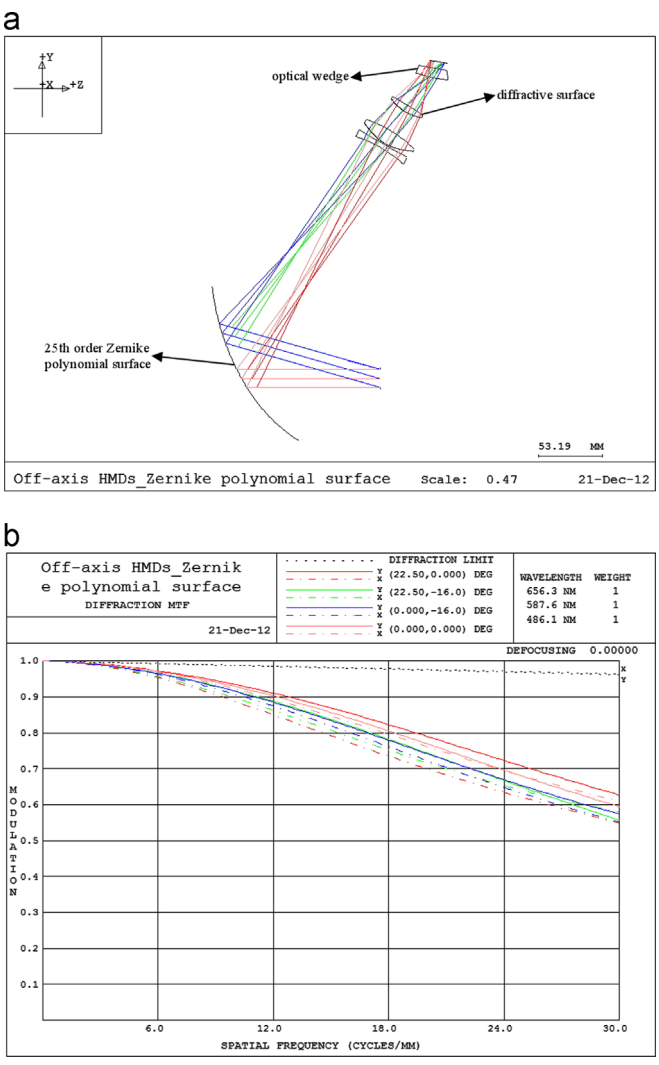

Fig. 3. (a) Optical layout of the off-axis HMDs with a combiner described by Zernike polynomial. (b) Polychromatic MTF plot of the off-axis HMDs.

the values of j and n.

$$l = floor\left[\frac{\sqrt{1+8i}-1}{2}\right],$$
$$n = i - l(l+1)/2,$$
$$j = l - n, \tag{12}$$

where floor( ) is integral operator. There are 14 terms used in the diffractive phase surface and it is the same with all the three designs in our paper.

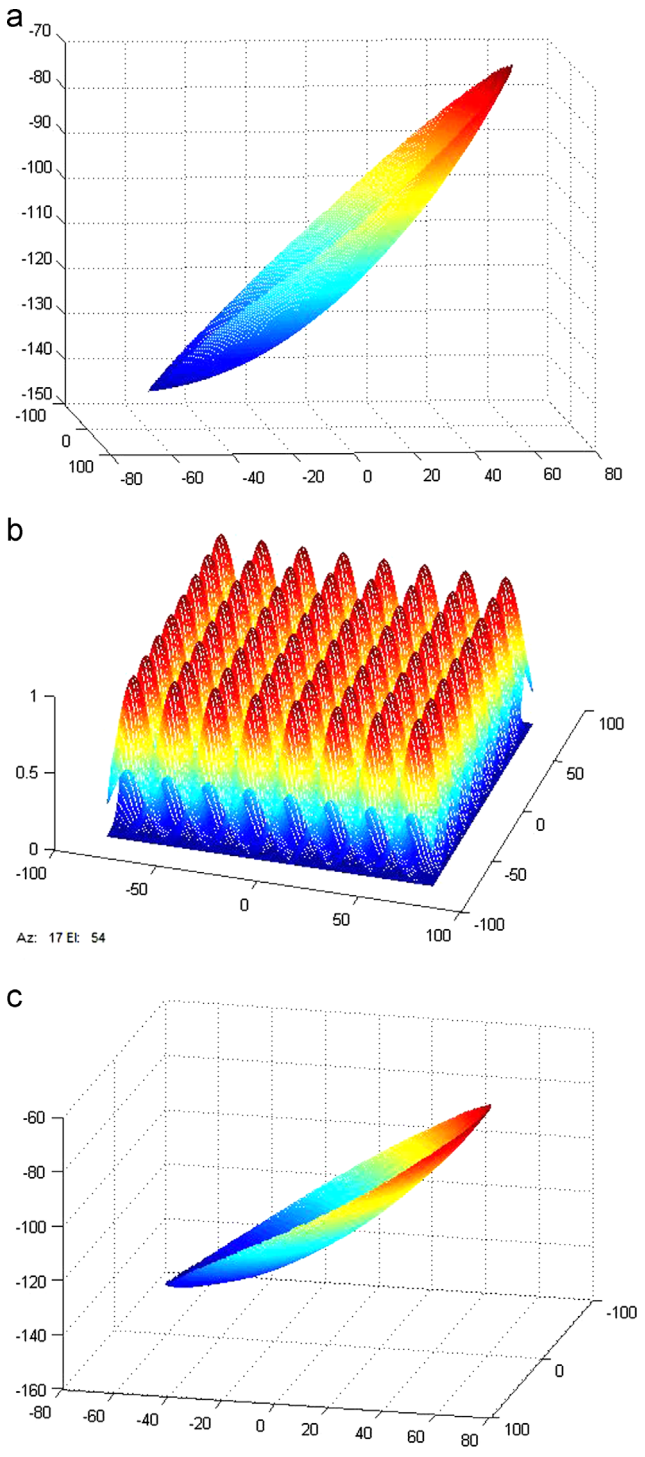

Fig. 4. (a) The shape of the combiner described with Zernike polynomial surface. (b) The basis functions are shown. The 2D Gaussians are spaced uniformly with means centered on an 8×8 grid. (c) The shape of the combiner described with the Gaussian radial basis functions.

The polychromatic diffraction MTF, plotted against the spatial frequency in cycles/mm, is shown in Fig. 2(b). From this MTF plot, a 33 lp/mm spatial frequency is shown that the MTF value at 0° field of view is greater than 0.5 and that is greater than 0.4 for all field view.

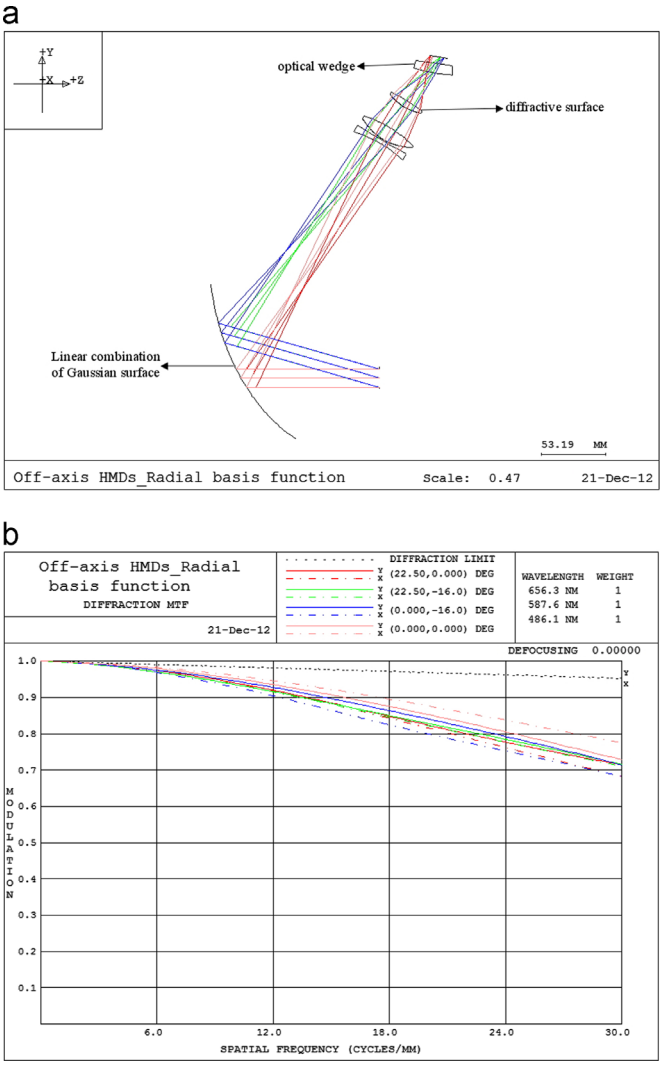

Fig. 5. (a) Optical layout of the off-axis HMDs with a combiner described by Gaussian radial basis functions. (b) Polychromatic MTF plot of the HMDs.

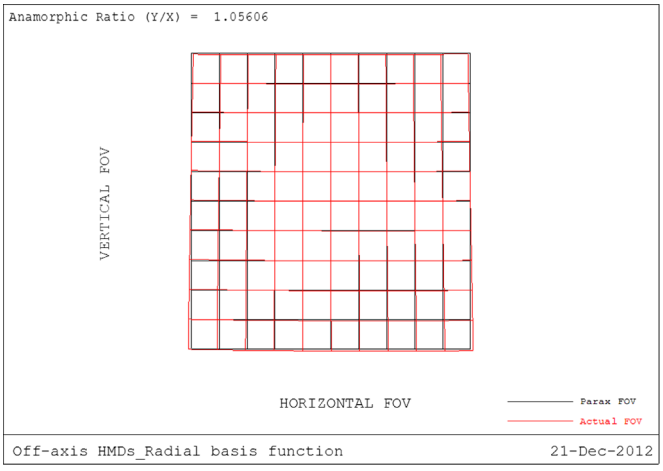

Fig. 6. Distortion grid comparing real and paraxial rays.

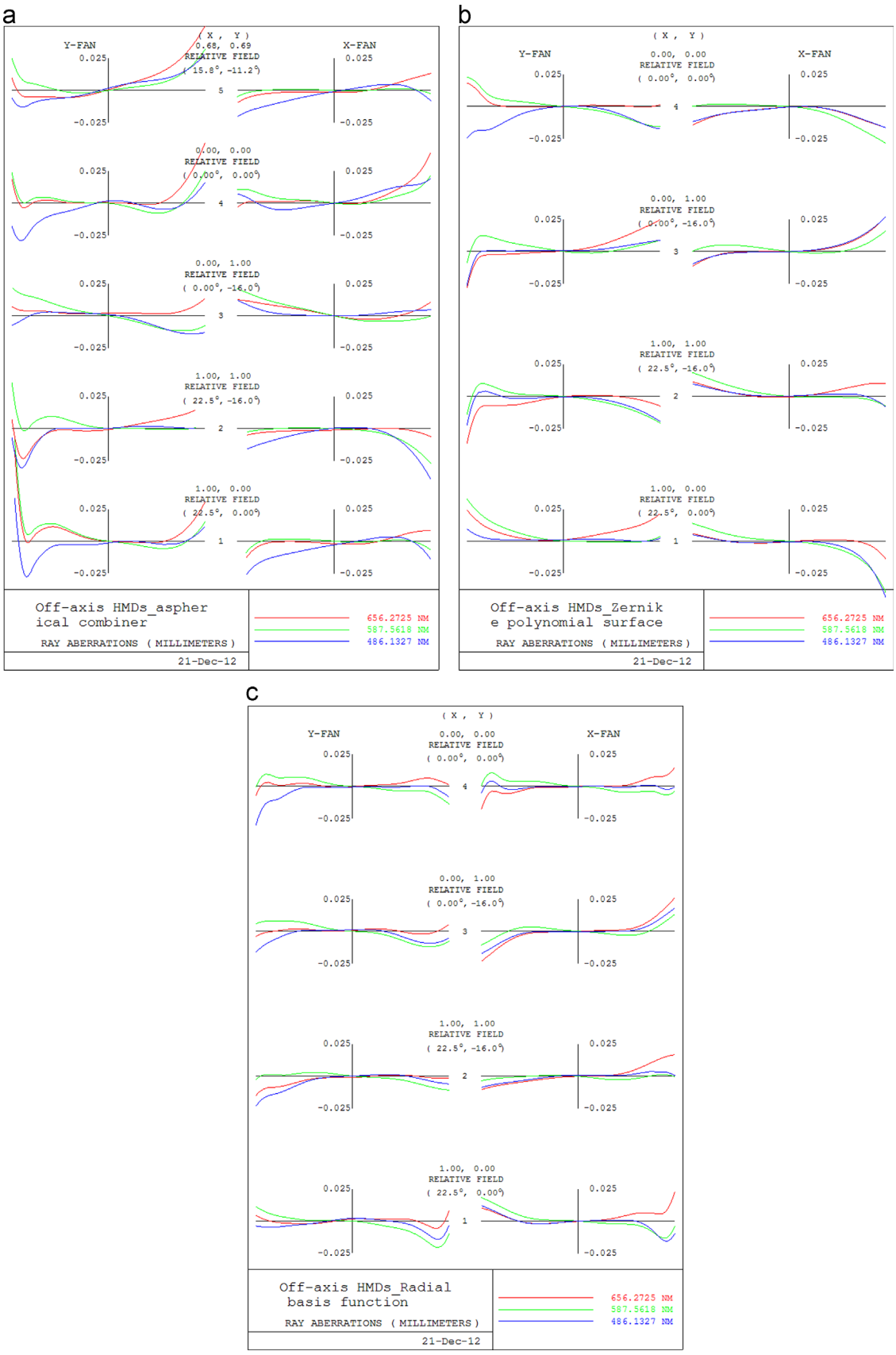

Fig. 7. Comparison of ray aberrations using (a) the aspheric surface, (b) the Zernike polynomial surface, and (c) Linear combination of Gaussians.

Another HMDs optical system which comprises a combiner and four relay lenses consisting of a negative lens, two biconvex lenses, and an optical wedge, arranged sequentially from the combiner to the image source is shown in Fig.3(a).

Based on the previous one, this HMDs have the same specifications as Table 1 too. However, what remains different is that the surface type of combiner changes from a 10th order asphere to a 25th order Zernike polynomial. The expression for Zernike polynomial is shown as the following:

$$z = \frac{cr^2}{1+\sqrt{1-(1+k)c^2r^2}} + \sum_{i=1}^{N} A_i Z_i, \tag{13}$$

Where z is the sagittal plane, k is the conic constant, c is the curvature of the surface, and r is the height above the optical axis; then $r^2 = x^2 + y^2$. A_i is the coefficient of the Zernike polynomial.

By changing the surface type, there are sharp differences in the structure of system between the two optical systems. First, the number of relay lenses changes from five to four, so the whole system has become much lighter in weight. Still, the distance between the combiner and the relay lens group becomes shorter, so it shortens the entire optical path and makes the HMDs have compact structure, suitable to the position of barycentre and convenient wearing. Of particular note is that the biconvex lens nearest to optical wedge is still a diffractive optical element. The performance of HMDs has been improved remarkably, which is shown in Fig. 3(b). By using the Zernike polynomial surface, an average MTF can achieve more than 50% at 33 line pairs/mm.

Next, we designed the HMDs optical system based on the design requirements as Table 1, the combiner of which was described with the Gaussian radial basis functions. We implemented the radial basis functions as a user-defined type 1 surface in the optical design software Code V® (software from Optical Research Associates, Pasadena, California) as a DLL (dynamically linked library). It is advisable to use the second HMDs optical system as the initial configuration when we start to design the optical system. In this case, we would try a new way to determine a starting point of optimization quickly. The optimization procedure is as follows. The first step was to get the expression of Zernike polynomial surface and it contains the specific coefficients. After getting the coefficients of the first 25 terms in Zernike polynomial from Code V®, we divided the aperture of combiner into x_m pieces in x-dimension and y_n pieces in y-dimension and then achieved the shape of the Zernike polynomial surface shown in fig. 4(a) via a fitting procedure of MATLAB. The second step was to determine the Gaussian radial basis functions. Specifically, we determined the input weight vector (i.e. the center of the Gaussian for node$i$) $\boldsymbol{\mu}_i$ and the normalization parameter σ_i^2 of Eq. (9). In this paper, the combiner surface is described by a uniformly spaced grid of 8×8 2D unit variance Gaussian functions which is shown in Fig. 4(b). The third step was to obtain the coefficients of the first 64 terms in the Gaussian functions. The Gaussian radial basis functions approximation to Zernike polynomial solved in step one was implemented by means of MATLAB, and then we got the coefficients of the first 64 terms in the Gaussian functions through least squares algorithm. The fourth step was to write a program in C++. By using link paths of Code V®, the edited program was compiled to the file of DLL that was added into the Code V's CVUSER subdirectory. The final step was to optimize the HMDs optical system through the use of the solved coefficients of the first 64 terms and the file of DLL. According to final optimization result, we obtain the shape of optical surface described with the Gaussian radial basis functions via a fitting procedure of MATLAB, which is shown in fig. 4(c).

The system was optimized by ray tracing from exit pupil to image source. The optimization constraints included the focal length, image distortion, and the space between combiner and relay lens group. The following parameters were set as variables, including all the primary curvatures of all the surfaces, the non-rotational symmetric polynomial coefficients up to y^4 describing the diffractive optical surface, aspheric coefficients, the image plane defocus, decenter in both Y and Z directions, tilt about the X axis, and the 64 weights for the 8×8 2D Gaussian basis functions.

The layout of the system is shown in Fig. 5(a); Fig. 5(b) shows the polychromatic diffraction MTF. From the MTF plot, 67% at the spatial frequency of 33 line pairs/mm is achieved across the full field using a combiner that is described with the Gaussian radial basis functions. Fig. 6 shows the appearance of a rectilinear grid as viewed through the HMDs and the maximum distortion is 3.2% at the bottom left and right corner of the field. Fig. 7 shows the comparison of ray aberration curves using an even aspheric surface, Zernike polynomial surface, and linear combination of Gaussians surface. Through Fig. 7(c), we can see that the use of radial basis functions can effectively reduce high-order off-axis aberration. The comparison of the properties between the linear combination of Gaussians surface and the other surface types is shown in Table 2.

Table 2
Comparison of the average tangential and sagittal MTF values and the number of relay lens between an asphere, Zernike polynomial, and a linear combination of Gaussians surface type.

Surface type	Average MTF (at 33 cycles/mm)	The number of relay lens
Asphere	40.8%	5
Zernike polynomial	55.1%	4
Linear combination of Gaussians	67.2%	4

4. Conclusion

With the introduction of the Gaussian radial basis functions to describe optical freeform surface, we have shown an off-axis see-through wide field of view HMDs with a 100 mm eye relief, 15 mm pupil, $45^\circ \times 32^\circ$ FOV, and 60° combiner tilt angle. The HMD was designed, analyzed, and compared to existing shape descriptors such as asphere and Zernike polynomial in this paper. From the results of comparison and analysis, we discovered that the use of linear combination of Gaussians surface on one hand could reduce the use count of optical element, simplify the structure of optical system and save weight. On the other hand, it could also get a higher level of modulation transfer function (MTF) performance. Specifically, there were one fewer optical element of relay lens group compared to an asphere and a 12.1% gain at the spatial frequency of 33 line pairs/mm compared to a Zernike polynomial. Furthermore, we tried a new maneuver to determine a starting point of optimization quickly while designing, and the finding suggests that it is helpful to design such optical system of user-defined surface.

References

[1] Albert B. Pratt, U.S. Patent 1, 183, 492, 1916.
[2] Jannick P. Rolland, Optical Engineering 39 (2000) 1760.
[3] Chen, C.W., U.S. Patent 5, 526, 183, 1996.
[4] Alex Cameron, Proceedings of SPIE 8383 (2012) 1.
[5] Z. Zheng, X. Liu, H. Liu, L. Xu, Applied Optics 49 (2010) 3661.
[6] I. Kaya, K.P. Thompson, J.P. Rolland, Optics Express 20 (2012) 22683.
[7] K. Fuerschbach, J.P. Rolland, K.P. Thompson, Optics Express 19 (2011) 21919.
[8] O. Cakmakci, B. Moore, H. Foroosh, J.P. Rolland, Optics Express 16 (2008) 1583.
[9] O. Cakmakci, S. Vo, H. Foroosh, J. Rolland, Optics Letters 33 (2008) 1237.
[10] M.D. Buhmann, Radial Basis Functions: Theory and Implementations, Cambridge University Press, Cambridge, United Kingdom, 2003.
[11] K.P. Thompson, Aberration Fields in Tilted and Decentered Optical Systems (Ph.D.thesis), University of Arizona, Tucson, Arizona, USA, 1980. (Ph.D. thesis).